Thus, insertion of a P element in the *Indy* gene may alter normal metabolism. In mammals, a moderate caloric restriction increases life-span, whereas a more severe restriction leads to starvation and decreased life-span (*27*). We postulate that the level of *Indy* expression is critical for life-span extension and that P-element insertions in *Indy* reduce Indy expression. When the level of Indy is mildly reduced, as in flies heterozygous for *Indy* insertions, there is a large extension in life-span. The extension in life-span is less dramatic with a further reduction in Indy activity, such as that seen in *Indy* homozygous flies, in which a 10 to 20% increase in mean life-span was seen (*12*). This model predicts that a further reduction in Indy activity would shorten life-span, and indeed this was observed when *Indy* gene activity was further reduced by placing an *Indy* mutation over a chromosome deleted for the *Indy* region. Flies with only a single copy of a mutant *Indy* gene and no normal copy of *Indy* (*Indy* mutant over deletion for the *Indy* region) had a 10 to 20% shorter mean and maximum life-span than did homozygous *Indy* mutants (*12*).

The mechanism by which caloric restriction mediates life-span extension is not understood, but it is likely to involve alterations in energy utilization. In contrast to many of the previously identified genes associated with life-span extension in metazoans, which have indirect effects on metabolism (*5–9*), *Indy* appears to be directly involved in intermediary metabolism and thus may represent a new class of longevity genes. A genetically induced reduction in the amount or efficiency of a dicarboxylic acid cotransporter in the *Indy* mutants may be creating a metabolic state similar to caloric restriction. Further characterization of the *Indy* mutants may provide direct genetic insight into the role of energy balance and aging, and a point of access for genetic and pharmacological interventions for extending life-span.

References and Notes

1. T. E. Johnson, *Science* **249**, 908 (1990).
2. C. J. Kenyon, E. Chang, A. Rudner, R. Tabtiang, *Nature* **366**, 461 (1993).
3. B. Lakowski, S. Hekimi, *Science* **272**, 1010 (1996).
4. K. D. Kimura, H. A. Tissenbaum, Y. Liu, G. Ruvkun, *Science* **277**, 942 (1997).
5. J. Z. Morris, H. A. Tissenbaum, G. Ruvkun, *Nature* **382**, 536 (1996).
6. S. Ogg *et al.*, *Nature* **389**, 994 (1997).
7. S. Hekimi, in *The Molecular Genetics of Aging, Results and Problems in Cell Differentiation*, S. Hekimi, Ed. (Springer-Verlag, New York, 2000), vol. 29, pp. 81–112.
8. H. M. Brown-Borg, K. E. Borg, C. J. Meliska, A. Bartke, *Nature* **384**, 33 (1996).
9. A. Bartke, in *The Molecular Genetics of Aging, Results and Problems in Cell Differentiation*, S. Hekimi, Ed. (Springer-Verlag, New York, 2000), vol. 29, pp. 181–202.
10. Y. J. Lin, L. Seroude, S. Benzer, *Science* **282**, 943 (1998).
11. S. Boynton, T. Tully, *Genetics* **131**, 655 (1992).
12. B. Rogina, R. A. Reenan, S. P. Nilsen, S. L. Helfand, data not shown.
13. E. Bier *et al.*, *Genes Dev.* **3**, 1273 (1989).
14. X. Z. Chen, C. Shayakul, U. V. Berger, W. Tian, M. A. Hediger, *J. Biol. Chem.* **273**, 20972 (1998).
15. A. M. Pajor, *Am. J. Phys.* **270**, F642 (1996).
16. ———, *Annu. Rev. Physiol.* **61**, 663 (1999).
17. M. J. Palladino, L. P. Keegan, M. A. O'Connell, R. A. Reenan, *Cell* **102**, 437 (2000).
18. V. B. Wigglesworth, *The Principles of Insect Physiology* (Chapman and Hill, London, ed. 7, 1972).
19. L. Sondergaard, *Trends Genet.* **9**, 193 (1993).
20. S. L. Helfand *et al.*, *Genetics* **140**, 549 (1995).
21. The FlyBase database of the *Drosophila* genome projects and community literature, *Nucleic Acids Res.* **27**, 85 (1999) (http://flybase.bio.indiana.edu/).
22. L. Luckinbill, R. Arking, M. J. Clare, W. C. Cirocco, S. Buck, *Evolution* **38**, 996 (1984).
23. L. Partridge, A. Green, K. Fowler, *J. Insect Physiol.* **33**, 745 (1987).
24. K. Fowler, L. Partridge, *Nature* **338**, 760 (1989).
25. R. S. Sohal, P. B. Buchan, *Exp. Gerontol.* **16**, 157 (1981).
26. M. R. Rose, *Evolutionary Biology of Aging* (Oxford Univ. Press, New York, 1991).
27. R. S. Sohal, R. Weindruch, *Science* **273**, 59 (1996).
28. Because genetic background has such a powerful effect on life-span, the genetic backgrounds of the lines being compared must be as similar as possible. The *Indy302* and *Indy206* mutants are both from the mutagenesis reported in (*11*), where an effort was made to use "Cantonized" stocks. In addition, each enhancer-trap line was further backcrossed to a Canton-S stock with the w^{1118} mutation multiple times (*11*). Our controls included four other enhancer-trap lines from the original mutagenesis (*11*), compared as heterozygotes with the same Canton-S stock as the *Indy302* and *Indy206* lines. The control for *Indy159* was similar; we compared another enhancer-trap line insertion from the same mutagenesis (*13*). The control line had an insert in the same cytological region as *Indy*, but not inserted into the *Indy* locus.
29. Single-letter abbreviations for the amino acid residues are as follows: A, Ala; C, Cys; D, Asp; E, Glu; F, Phe; G, Gly; H, His; I, Ile; K, Lys; L, Leu; M, Met; N, Asn; P, Pro; Q, Gln; R, Arg; S, Ser; T, Thr; V, Val; W, Trp; and Y, Tyr.

30. We thank J. Jack, B. Graveley, and M. Tanzer for helpful discussions. Supported by grants from the NIH-supported Claude Pepper Older Americans Independence Center at the University of Connecticut Center on Aging and the American Federation for Aging Research (B.R.); by NSF grant 9728737 and a grant from The Patrick and Catherine Weldon Donaghue Medical Research Foundation (R.A.R); and by the National Institute on Aging (grants AG14532 and AG16667), a Burroughs Wellcome Travel Grant, and a Donaghue Investigator Award from The Patrick and Catherine Weldon Donaghue Medical Research Foundation (S.L.H).

17 October 2000; accepted 14 November 2000

Docosahexaenoic Acid, a Ligand for the Retinoid X Receptor in Mouse Brain

Alexander Mata de Urquiza,[1] Suya Liu,[2]* Maria Sjöberg,[3]* Rolf H. Zetterström,[1] William Griffiths,[2] Jan Sjövall,[2] Thomas Perlmann[1]†

The retinoid X receptor (RXR) is a nuclear receptor that functions as a ligand-activated transcription factor. Little is known about the ligands that activate RXR in vivo. Here, we identified a factor in brain tissue from adult mice that activates RXR in cell-based assays. Purification and analysis of the factor by mass spectrometry revealed that it is docosahexaenoic acid (DHA), a long-chain polyunsaturated fatty acid that is highly enriched in the adult mammalian brain. Previous work has shown that DHA is essential for brain maturation, and deficiency of DHA in both rodents and humans leads to impaired spatial learning and other abnormalities. These data suggest that DHA may influence neural function through activation of an RXR signaling pathway.

The nuclear hormone receptors are ligand-activated transcription factors [reviewed in (*1*)]. Included in this family are the so-called "orphan receptors," whose ligands have not been identified [reviewed in (*1, 2*)]. By screening chemical libraries, progress has been made in identifying ligands for these receptors [for examples, see (*3–8*)]; however, in most cases endogenous ligands have remained elusive.

[1]Ludwig Institute for Cancer Research, Stockholm Branch, Box 240, S-171 77 Stockholm, Sweden. [2]Department of Medical Chemistry and [3]Department of Cell and Molecular Biology, Karolinska Institutet, S-171 77 Stockholm, Sweden.

*These authors contributed equally to this work.
†To whom correspondence should be addressed. E-mail: thomas.perlmann@licr.ki.se

RXR is an obligatory component of a large number of nuclear receptor heterodimers and is activated in vitro by the vitamin A metabolite 9-*cis* retinoic acid (9-*cis* RA), which binds with high affinity to the RXR ligand binding domain (*9, 10*); however, 9-*cis* RA acid has been difficult to detect in vivo (*11*). Nonetheless, because numerous studies have demonstrated striking synergism in biological responses in vitro and in vivo when both partners of the RXR-RAR heterodimer are activated by their respective ligand [for examples, see (*12–14*)], it seems likely that ligand-induced activation of RXR does occur in vivo. This conclusion has been corroborated by experiments with transgenic mice (*15, 16*).

To search for endogenous ligands that acti-

vate retinoid receptors RAR and RXR, we used a cell-based reporter gene assay. Human chorion carcinoma JEG-3 cells were co-transfected with an upstream activating sequence (UAS) luciferase reporter construct and either GAL4-RAR or GAL4-RXR expression vectors encoding the yeast GAL4 DNA-binding domain fused to the ligand-binding domains of human (h) RARα and hRXRα, respectively (*17*). The cells were then cultured with serum-free media that had been incubated overnight with various tissues from embryonic or adult mice (*18*). Consistent with previous studies, we found that media conditioned with brain tissue from embryonic day 13.5 (E13.5) embryos activated RAR but not RXR (Fig. 1A) (*11*). In contrast, media conditioned with adult brain tissue activated RXR but not RAR (Fig. 1A). The RXR-activating factor(s) were present in hippocampus, striatum, motor cortex, and cerebellum, but not in spinal cord (*19*).

Two lines of evidence indicated that the adult brain-conditioned medium directly activated RXR rather than an RXR heterodimerizing partner expressed in JEG-3 cells. First, an RXR-specific antagonist (LG849) (*15*) abolished reporter gene expression, and an RAR-specific antagonist had no effect (Fig. 1B). Second, the brain-conditioned medium activated RXR when RXR heterodimerized with the orphan receptor Nurr1 (*20, 21*). Thus, when GAL4-Nurr1 was expressed as a bait, potent activation was observed only in cells co-transfected with RXR expression vector (Fig. 1C). Again, activation was abolished by the RXR-specific antagonist LG849.

To identify the RXR-activating factor(s), we extracted the brain-conditioned medium with hexane (*22*) and found that the activity was present in the hexane extracts, consistent with the possibility that the activating factor is a lipophilic molecule (Fig. 2A). Acidification of the medium with hydrochloric acid increased the yield, indicating that the active substance is a lipophilic, negatively charged molecule (Fig. 2A).

We purified the activity to homogeneity by two cycles of high-performance liquid chromatography (HPLC) (Fig. 2, B and C) (*22*). Redissolved hexane extract was initially fractionated by normal-phase HPLC, and individual fractions were assayed in transfected JEG-3 cells. The fractions containing the activity were then pooled and separated by reversed-phase HPLC. The peak fractions were analyzed by negative-ion nano-electrospray (nano-ES) mass spectrometry (Fig. 3A)

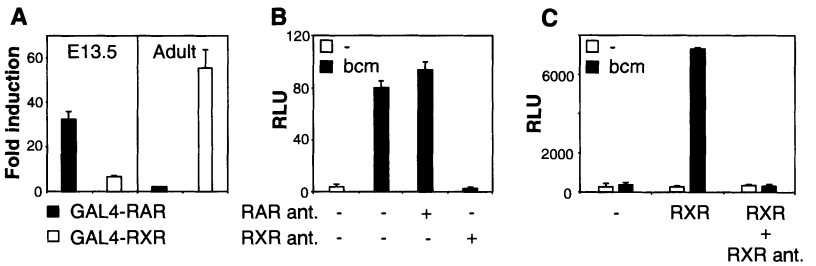

Fig. 1. RXR-specific activation by factor(s) enriched in adult brain. (**A**) JEG-3 cells were transfected with a luciferase reporter plasmid containing four UAS binding sites (UASx4-tk-luc) and either GAL4-RARα or GAL4-RXRα expression vectors, followed by treatment with conditioned medium as depicted. Values are shown as fold induction after normalization to β-galactosidase (β-gal). (**B**) JEG-3 cells transfected with GAL4-RXR expression vector and UASx4-tk-luc reporter were incubated with brain-conditioned medium (bcm) in the presence or absence of RXR-specific (LG849) or RAR-specific antagonists (RO41-5253). Values are shown as relative light units (RLU) after normalization to β-gal. (**C**) JEG-3 cells were transfected with GAL4-Nurr1 expression vector alone or in combination with RXR expression vector. The cells were then incubated with brain conditioned medium, with or without an RXR-specific antagonist [see (B)]. Values are shown as RLU after normalization to β-gal.

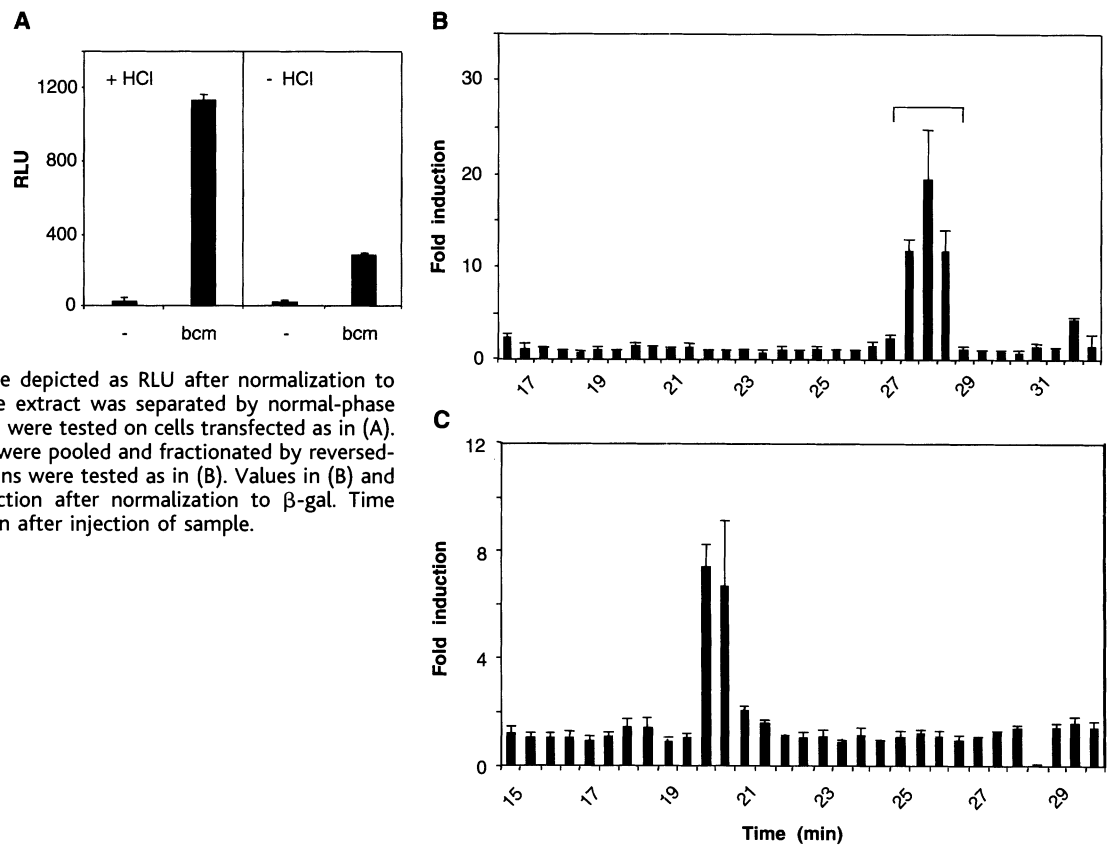

Fig. 2. Purification of activating factor from brain-conditioned medium. (**A**) Brain-conditioned medium was extracted with hexane in the presence (left) or absence (right) of 0.1 M hydrochloric acid (final concentration). Evaporized hexane extracts were redissolved in a small volume of ethanol, and aliquots were added to cultured JEG-3 cells transfected with UASx4-tk-luc reporter and GAL4-Nurr1 and RXR expression vectors. Values are depicted as RLU after normalization to β-gal. (**B**) Redissolved hexane extract was separated by normal-phase HPLC, and individual fractions were tested on cells transfected as in (A). (**C**) Active fractions from (B) were pooled and fractionated by reversed-phase HPLC. Individual fractions were tested as in (B). Values in (B) and (C) are shown as fold induction after normalization to β-gal. Time corresponds to time of elution after injection of sample.

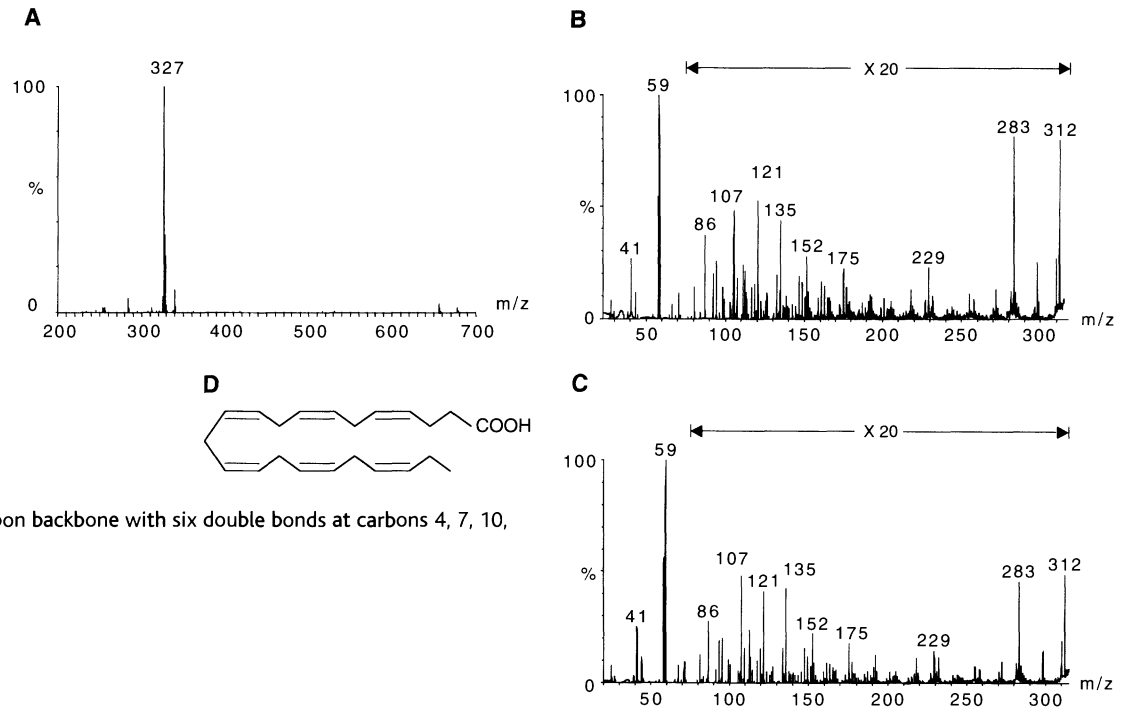

Fig. 3. Identification of DHA as a brain-derived RXR-activating factor. (**A**) Peak fractions from the reversed-phase HPLC were analyzed by mass spectrometry, recording negative-ion nano-ES spectra. The active fraction is dominated by a very intense peak at *m/z* 327.2. Minor peaks are observed at *m/z* 283.2, 339.2, and 655.5, the latter consisting of dimers of the *m/z* 327.2 ion. (**B** and **C**) Collision-induced dissociation spectra of the $[M-H]^-$ ion of the ion at *m/z* of 327.2 from the active fraction (B) and the reference fatty acid *cis*-4,7,10,13,16,19-DHA (C) were recorded and compared. (**D**) DHA has a 22-carbon backbone with six double bonds at carbons 4, 7, 10, 13, 16, and 19.

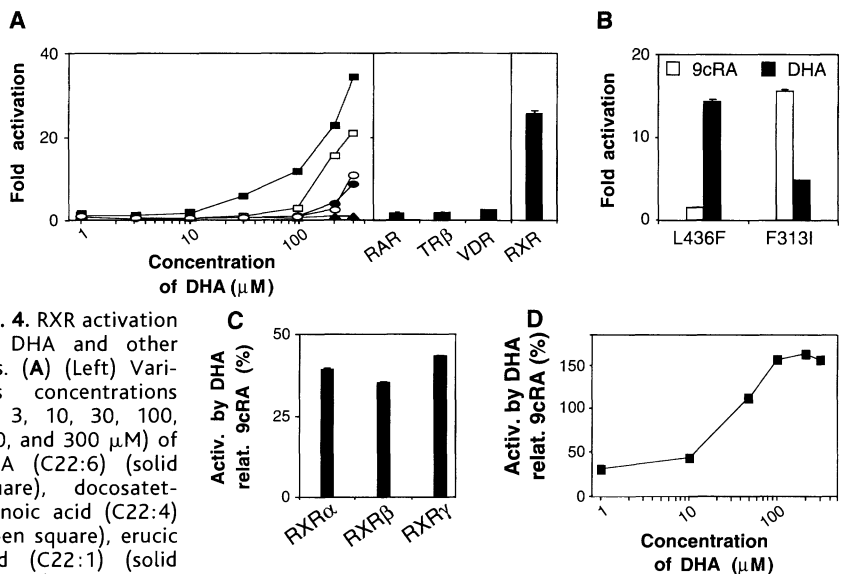

Fig. 4. RXR activation by DHA and other FAs. (**A**) (Left) Various concentrations (1, 3, 10, 30, 100, 200, and 300 μM) of DHA (C22:6) (solid square), docosatetraenoic acid (C22:4) (open square), erucic acid (C22:1) (solid triangle), arachidonic acid (C20:4) (solid circle), and oleic acid (C18:1) (open circle) were titrated on 293T cells transfected with CMX-RXRα expression vector and Apo-A1-tk-luc reporter. Values are shown as fold induction after normalization to β-gal. (Right) 293T cells were transfected with UASx4-tk-luc reporter and either CMX-GAL4-RARα, CMX-GAL4-TRβ, CMX-GAL4-VDR, or CMX-GAL4-RXRα expression vectors, and treated with 100 μM DHA. The results are depicted as fold activation after normalization to β-gal. (**B**) 293T cells were transfected with Apo-A1-tk-luc reporter and either CMX-RXRα F313I or CMX-RXRα L436F expression vectors, and then treated with 9-*cis* RA (0.1 μM) or DHA (33 μM). Values are shown as fold activation after normalization to β-gal. (**C**) 293T cells were transfected with Apo-A1-tk-luc reporter and either CMX-RXRα, CMX-RXRβ, or CMX-RXRγ, followed by treatment with 9-*cis* RA (0.1 μM) or DHA (150 μM). Values are shown as percent of activation reached by 9-*cis* RA. (**D**) Various concentrations (1, 10, 50, 100, 200, and 300 μM) of DHA were titrated on 293T cells transfected with UASx4-tk-luc reporter and GAL4-Nurr1 and RXR expression vectors. Values are shown as percent of activation reached by 0.1 μM 9-*cis* RA.

(*23*). The spectrum of the active fraction was dominated by an intense ion at a mass-to-charge ratio (*m/z*) of 327.2; there were minor peaks at *m/z* of 283.2, 339.2, and 655.5. From this analysis, we concluded that the molecular formula of the active compound is $C_{22}H_{32}O_2$, similar to that of the polyunsaturated fatty acid (PUFA) docosahexaenoic acid (DHA). Collision-induced dissociation spectra recorded of the ion at *m/z* 327.2 (Fig. 3B) and the $[M-H]^-$ ion of *cis*-4,7,10,13,16,19-DHA confirmed this conclusion (Fig. 3C). Thus, the major purified component is *cis*-4,7,10,13,16,19-DHA.

To confirm that DHA is the active compound, we tested DHA and several other PUFAs for their ability to activate a reporter gene responsive to wild-type RXR in human embryonic kidney 293T cells co-transfected with an expression vector for wild-type hRXRα. In dose-response studies, DHA was the most efficient activator with an EC_{50} (median effective concentration) at ~50 to 100 μM (Fig. 4A) (*17, 24*). Docosatetraenoic acid (C22:4*cis*7,10,13,16), a PUFA that is structurally related to DHA, induced activation at concentrations approximately 5 to 10 times higher, whereas arachidonic acid (C20:4*cis*5,8,11,14) and oleic acid (C18:1*cis*9) induced activation only at the highest concentration tested (330 μM) (Fig. 4A). No activation was induced by erucic acid (C22:1*cis*13) (Fig. 4A), unsaturated C22, or various C18, C20, C21, C22, and C23 monounsaturated fatty acids, and only weak activation was induced by C18:2, C18:3, C22:3, and C22:5 (*25*). DHA was specific for RXR; DHA did not activate RAR, the thyroid hormone receptor (TR), or the vitamin D receptor (VDR) (Fig. 4A). Furthermore, activation by DHA was sensitive to mutations that alter the ligand-binding specificity of RXR (*26*), indicating that DHA activates RXR by a true ligand-binding mechanism (Fig. 4B). We next tested the maximal response compared

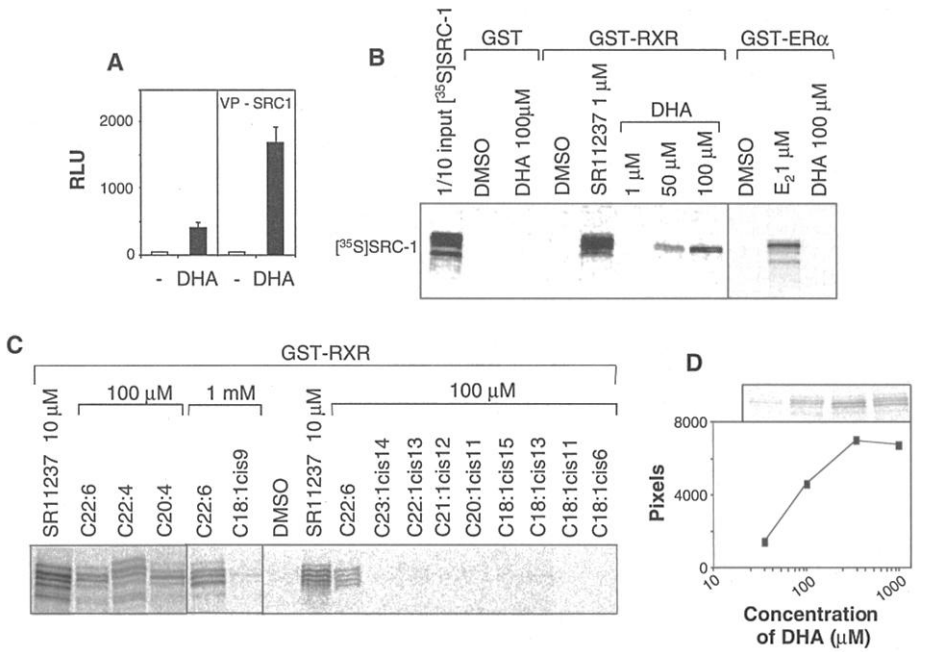

Fig. 5. DHA mediates RXR/SRC-1 interaction in vivo and in vitro. (**A**) 293T cells were transfected with UASx4-tk-luc reporter and either CMX-GAL4-RXR alone or in combination with VP16-SRC-1. The cells were incubated with serum-free medium or medium containing 33 μM DHA. Values are shown as RLU after normalization to β-gal. (**B**) Bacterially expressed GST fusion proteins of hRXRα and mouse ERα ligand-binding domains were bound to glutathione-Sepharose beads and incubated overnight with [^{35}S]SRC-1 in the presence of vehicle, 1 μM SR11237, DHA, or 1 μM estradiol. (**C**) Bacterially expressed GST fusion protein of human RXRα ligand-binding domain was bound to glutathione-Sepharose beads and incubated overnight with [^{35}S]SRC-1 protein in the presence of vehicle, 10 μM SR11237, or 100 μM or 1 mM concentrations of the indicated fatty acids. (**D**) Interaction of bacterially expressed GST fusion RXR and [^{35}S]SRC-1 proteins was analyzed in the presence of DHA. Quantification was performed using a PhosphorImager.

to that of 9-*cis* RA using RXRα, RXRβ, and RXRγ. All three isotypes were activated by 150 μM DHA, but activation was only at 40 to 45% the level seen with 0.1 μM 9-*cis* RA (Fig. 4C). Interestingly, lower concentrations of DHA were 1.5 times more potent than 0.1 μM 9-*cis* RA in activating GAL4-Nurr1/RXR (Fig. 4D), suggesting that RXR's heterodimerization partner may significantly affect its responsiveness to DHA.

To determine whether DHA is a ligand for RXR, we performed experiments with the steroid receptor coactivator 1 (SRC-1) (*27*). In transfected cells, DHA promoted interaction between RXR and SRC-1 (Fig. 5A). Moreover, DHA bound to the ligand-binding domain of RXR in vitro, as shown by a GST pull-down experiment in which the bacterially expressed ligand-binding domain of RXR interacted with [^{35}S]SRC-1 in the presence but not in the absence of DHA (Fig. 5B) (*28*). A fusion of GST with the estrogen receptor α LBD (GST-ER) did not interact with SRC-1, either in the presence or absence of DHA (Fig. 5B). Consistent with the activation data, some interaction between RXR and SRC-1 was observed in the presence of docosatetraenoic acid (C22:4) and arachidonic acid (C20:4) (Fig. 5C). Oleic acid (C18:1*cis*9) and other tested fatty acids (C23:1*cis*14, C22:1*cis*13, C21:1*cis*12, C20:1*cis*11, C18:1*cis*15, C18:1*cis*13, C18:1*cis*11, and C18:1*cis*6) induced only very weak or no interaction (Fig. 5C). DHA induced SRC-1 interaction with RXR at concentrations consistent with the activation profile observed in transfected cells (Figs. 4A and 5D). Thus, DHA can activate RXR and bind directly to the ligand-binding domain of this nuclear receptor. Interestingly, it was recently reported that crystals of a mutated derivative of the RXR ligand-binding domain contain oleic acid (*29*), suggesting a structural basis for how fatty acids and their derivatives may interact with RXR in vivo.

RXR has also been shown to be activated in transfected cells by high concentrations of phytanic acid, a toxic chlorophyll metabolite, but this compound is eliminated from tissues in vivo (*30*). In contrast, DHA constitutes as much as 30 to 50% of total FAs in the mammalian brain, where it is predominantly associated with membrane phospholipids [reviewed in (*31, 32*)]. Thus, high levels of DHA are localized in the brain and the amount of free DHA could be significantly increased by release of a minor fraction of the membrane-bound DHA. Indeed, previous studies have demonstrated an autocrine phospholipase A_2– and phospholipase C–mediated release of DHA from phospholipids, e.g., in response to neurotransmitters (*33*) and after brain injury (*34*). Alternatively, DHA may be released and activate RXR in neighboring cells in a paracrine fashion. Indeed, it has been suggested that brain astrocytes supply neurons with DHA (*35*).

DHA becomes highly enriched in the mammalian brain during late gestation and early postnatal development [reviewed in (*31*)] and is essential for brain maturation both in rodents and humans [reviewed in (*31, 32, 36*)]. High levels of DHA accumulate in the retina, a tissue that develops abnormally in RXRα knock-out mice (*37*). DHA deficiency in rats and humans results in impaired spatial learning as well as other abnormalities (*38–40*), and, interestingly, similar learning defects are seen in RXRγ-deficient mice (*41*). DHA and other PUFAs also exert profound effects on metabolism and energy homeostasis [reviewed in (*42*)]. DHA is a major constituent of nutrients rich in ω3 PUFAs and has beneficial effects on blood cholesterol levels and insulin sensitivity [reviewed in (*42, 43*)]. Synthetic RXR ligands have similar influences in mice and humans, suggesting that RXR activation may contribute to effects achieved by dietary intake of ω3 PUFAs (*44–46*). Several RXR heterodimerization partners such as peroxisome proliferator-activated receptors, the liver X receptors and farnesoid X receptor are essential for regulating energy and nutritional homeostasis in response to their respective ligands [reviewed in (*47, 48*)]. An intriguing possibility is that DHA modulates these and other regulatory events by binding to the RXR subunit of nuclear receptor heterodimers.

References and Notes

1. D. J. Mangelsdorf *et al.*, *Cell* **83**, 835 (1995).
2. V. Giguère, *Endocr. Rev.* **20**, 689 (1999).
3. L. Nagy, P. Tontonoz, J. G. Alvarez, H. Chen, R. M. Evans, *Cell* **93**, 229 (1998).
4. M. Makishima *et al.*, *Science* **284**, 1362 (1999).
5. D. J. Parks *et al.*, *Science* **284**, 1365 (1999).
6. H. Wang, J. Chen, K. Hollister, L. C. Sowers, B. M. Forman, *Mol. Cell* **3**, 543 (1999).
7. S. A. Kliewer *et al.*, *Cell* **92**, 73 (1998).
8. B. Blumberg *et al.*, *Genes Dev.* **12**, 3195 (1998).
9. R. A. Heyman *et al.*, *Cell* **68**, 397 (1992).
10. A. A. Levin *et al.*, *Nature* **355**, 359 (1992).
11. C. Horton, M. Maden, *Dev. Dyn.* **202**, 312 (1995).
12. J. Botling, D. S. Castro, F. Oberg, K. Nilsson, T. Perlmann, *J. Biol. Chem.* **272**, 9443 (1997).
13. H. C. Lu, G. Eichele, C. Thaller, *Development* **124**, 195 (1997).
14. B. Roy, R. Taneja, P. Chambon, *Mol. Cell. Biol.* **15**, 6481 (1995).
15. L. Solomin *et al.*, *Nature* **395**, 398 (1998).
16. B. Mascrez *et al.*, *Development* **125**, 4691 (1998).
17. Cells were transfected in triplicate in 24-well plates by the calcium phosphate method (*20*). The cells were harvested 24 hours later, and the extracts were assayed for luciferase and reference β-galactosidase activity in a microplate luminometer/photometer reader (Lucy-1; Anthos, Salzburg, Austria).
18. Adult (6 to 8 weeks) wild-type (NMRI) male mice were perfused via the ascending aorta with cold phosphate-buffered saline. Organs were dissected, cut into small pieces, and placed in cell culture medium (MEM). Embryonal (E13.5) tissues were collected from wild-type (NMRI) embryos as above. Tissues were incubated with the medium overnight at 37°C.

This conditioned medium was then separated from the tissue and frozen.
19. Supplemental Web material may be found at www.sciencemag.org/cgi/content/full/290/5499/2140/DC1.
20. T. Perlmann, L. Jansson, *Genes Dev.* **9**, 769 (1995).
21. B. M. Forman, K. Umesono, J. Chen, R. M. Evans, *Cell* **81**, 541 (1995).
22. Conditioned medium was acidified with hydrochloric acid, mixed with an equal volume of hexane, and shaken vigorously for 5 min. This mixture was centrifuged, and the upper organic phase was recovered. Extraction of the aqueous phase was repeated once. The hexane extract was evaporated under nitrogen gas, and for activity assays, the residue was redissolved in 100 to 200 μl of ethanol. Hexane extract of conditioned medium was evaporated, redissolved in hexane, and injected onto a normal-phase HPLC column (Genesis Silica 4-μm particle size, 4.6 mm by 25 cm, Jones Chromatography Ltd., UK). Elution was performed using a linear gradient from hexane to hexane/dichloromethane/isopropanol (85:10:5, v/v), both containing 1% acetic acid, in 30 min at a flow rate of 0.5 ml/min. Starting 17 min after injection, 30 fractions containing 0.25 ml each, were collected. Active fractions were pooled, evaporated, and redissolved in 50 μl 80% methanol. We injected 30 μl onto a reversed-phase HPLC column (Genesis C18, 4-μm particle size, 3.0 mm by 25 cm). A mobile phase of methanol/isopropanol/water (80:10:10, v/v) containing 1% acetic acid at a flow rate of 0.3 ml/min was used. Active fractions along with the preceding and subsequent fractions were analyzed by nano-ES mass spectrometry.
23. Negative-ion nano-ES spectra were recorded on a AutoSpec-OATOFFPD (Micromass, Manchester, UK) hybrid double focusing magnetic sector–orthogonal acceleration (OA) time-of-flight (TOF) tandem mass spectrometer focal plane detector (FPD). Mass spectra were recorded as magnet scans over an *m/z* range of 70 to 1000 at an instrument resolution of 3000 (10% valley definition). Collision-induced dissociation (CID) spectra were recorded by selecting the precursor $[M-H]^-$ ions with the double-focusing sectors of the instrument, and focusing them into the fourth field–free region gas cell containing xenon collision gas. Undissociated precursor ions and fragment ions were pulsed into an OATOF mass analyzer.
24. All fatty acid ligands were purchased from Sigma, except C21:1*cis*12 and C23:1*cis*14, which were purchased from Nu-Chek-Prep (Elysian, MN).
25. A. Mata de Urquiza *et al.*, data not shown.
26. D. J. Peet, D. F. Doyle, D. R. Corey, D. J. Mangelsdorf, *Chem. Biol.* **5**, 13 (1998).
27. S. A. Oñate, S. Y. Tsai, M.-J. Tsai, B. W. O'Malley, *Science* **270**, 1354 (1995).
28. Bacterially expressed glutathione *S*-transferase (GST) or GST fusion proteins were bound to glutathione-Sepharose 4B beads (Pharmacia Biotech). SRC-1 cDNA was used to generate [^{35}S]methionine-labeled proteins (*49*). The labeled proteins were incubated with beads containing GST or GST fusion proteins in the presence of dimethyl sulfoxide (DMSO), DHA, or 1 μM estradiol. After an overnight incubation, free proteins were washed away. Bound proteins were eluted in loading buffer, separated by SDS–polyacrylamide gel electrophoresis, and visualized by fluorography.
29. W. Bourguet *et al.*, *Mol. Cell* **5**, 289 (2000).
30. S. Kitareewan *et al.*, *Mol. Biol. Cell* **7**, 1153 (1996).
31. M. Neuringer, G. J. Anderson, W. E. Connor, *Annu. Rev. Nutr.* **8**, 517 (1988).
32. N. Salem Jr., H.-Y. Kim, J. A. Yergey, in *Health Effects of Polyunsaturated Fatty Acids in Seafoods*, A. P. Simopoulos, R. R. Kifer, R. E. Martin, Eds. (Academic Press, New York, 1986), chap. 15, pp. 263–317.
33. M. C. Garcia, H.-Y. Kim, *Brain Res.* **768**, 43 (1997).
34. P. Homayoun *et al.*, *Neurochem. Res.* **25**, 269 (2000).
35. A. A. Spector, *Lipids* **34**, S1 (1999).
36. M. Makrides, M. Neumann, K. Simmer, J. Pater, R. Gibson, *Lancet* **345**, 1463 (1995).
37. P. Kastner *et al.*, *Cell* **78**, 987 (1994).
38. S. Gamoh *et al.*, *Neuroscience* **93**, 237 (1999).
39. R. Sheaff Greiner, T. Moriguchi, A. Hutton, B. M. Slotnick, N. Salem Jr., *Lipids* **34**, S239 (1999).
40. J. D. Fernstrom, *Lipids* **34**, 161 (1999).
41. M.-Y. Chiang *et al.*, *Neuron* **21**, 1353 (1998).
42. L. H. Storlien, A. J. Hulbert, P. L. Else, *Curr. Opin. Clin. Nutr. Metab. Care* **1**, 559 (1998).
43. D. P. Rose, J. M. Connolly, *Pharmacol. Ther.* **83**, 217 (1999).
44. J. J. Repa *et al.*, *Science* **289**, 1524 (2000).
45. R. Mukherjee *et al.*, *Nature* **386**, 407 (1997).
46. E. D. Bischoff, M. M. Gottardis, T. E. Moon, R. A. Heyman, W. W. Lamph, *Cancer Res.* **58**, 479 (1998).
47. T. M. Willson, P. J. Brown, D. D. Sternbach, B. R. Henke, *J. Med. Chem.* **43**, 527 (2000).
48. A. Chawla, E. Saez, R. M. Evans, *Cell* **103**, 1 (2000).
49. V. Cavaillés, S. Dauvois, P. S. Danielian, M. G. Parker, *Proc. Natl. Acad. Sci. U.S.A.* **91**, 10009 (1994).
50. We thank R. Heyman and R. Bissonnette for LG849, L. Foley for SR11237, D. Mangelsdorf for plasmids encoding RXRL436F and RXRF313I derivatives, L. Solomin for helpful comments on this manuscript, and members of the Perlmann lab for valuable discussion. Supported by the Human Frontiers Science Program, the Göran Gustafssons Foundation, and the Swedish Medical Research Council grant 03X-12551 (S.L., W.G., and J.S.), the Swedish Wennergren Foundation (M.S.), and the Swedish Cancer Society (M.S.).

26 May 2000; accepted 14 November 2000

Global Analysis of the Genetic Network Controlling a Bacterial Cell Cycle

Michael T. Laub,[1] Harley H. McAdams,[1] Tamara Feldblyum,[2] Claire M. Fraser,[2] Lucy Shapiro[1]*

This report presents full-genome evidence that bacterial cells use discrete transcription patterns to control cell cycle progression. Global transcription analysis of synchronized *Caulobacter crescentus* cells was used to identify 553 genes (19% of the genome) whose messenger RNA levels varied as a function of the cell cycle. We conclude that in bacteria, as in yeast, (i) genes involved in a given cell function are activated at the time of execution of that function, (ii) genes encoding proteins that function in complexes are coexpressed, and (iii) temporal cascades of gene expression control multiprotein structure biogenesis. A single regulatory factor, the CtrA member of the two-component signal transduction family, is directly or indirectly involved in the control of 26% of the cell cycle–regulated genes.

In the bacterium *Caulobacter crescentus*, a complex genetic network controls essential cell cycle functions, including the ordered biogenesis of structures at the cell poles and division plane (*1*). Because different functions occur at specific times in the *Caulobacter* cell cycle (Fig. 1A), regulation of the cell cycle must be examined as an integrated system. The availability of the full *Caulobacter* genome sequence and microarray gene expression assays now allow such an approach.

To determine the contribution of transcriptional control to bacterial cell cycle progression, we constructed DNA microarrays containing 2966 predicted open reading frames, representing about 90% of all *Caulobacter* genes (*2*). More than 19% of the *Caulobacter* genes exhibited discrete times of transcriptional activation and repression during a normal cell cycle. Prokaryotic biology has focused on external, environmental cues as the major mechanism for turning bacterial genes on and off, rather than internal cues. Surprisingly, the transcription of genes required for many cell cycle functions, such as DNA replication, chromosome segregation, and cell division, occurred just before or nearly coincident with the time of execution of that function, paralleling temporal patterns of gene expression observed in the yeast cell cycle (*3, 4*).

Swarmer cells from wild-type *C. crescentus* were isolated and allowed to proceed synchronously through their 150-min cell cycle (Fig. 1A). RNA was harvested from cell samples taken at 15-min intervals. RNA levels for each gene at each time point were compared to RNA levels in a mixed, unsynchronized reference population by means of microarrays (*5*). To determine which RNAs varied as a function of the cell cycle, we used a discrete cosine transform algorithm to identify expression profiles that varied in a cyclical manner (*5*). This analysis identified 553 genes whose RNA levels changed as a function of the cell cycle. The 72 genes with previously characterized cell cycle–regulated promoters were in this set of temporally regulated transcripts, and they exhibited peak times of expression consistent with earlier data (*5*).

A self-organizing map clustering technique was applied to the 553 cell cycle–

[1]Department of Developmental Biology, Beckman Center, Stanford University School of Medicine, Stanford, CA 94305, USA. [2]The Institute for Genomic Research, 9712 Medical Center Drive, Rockville, MD 20850, USA.

*To whom correspondence should be addressed. E-mail: shapiro@cmgm.stanford.edu